



ELSEVIER

Available online at www.sciencedirect.com

SCIENCE @ DIRECT®

JOURNAL OF
CONSTRUCTIONAL
STEEL RESEARCH

Journal of Constructional Steel Research 59 (2003) 1057–1082

www.elsevier.com/locate/jcsr

Hysteresis behavior of semi-rigid double web angle steel connections

A. Abolmaali ^{a,*}, A.R. Kukreti ^b, H. Razavi ^a

^a *Department of Civil and Environmental Engineering, University of Texas at Arlington, PO Box 19308, Arlington, TX, USA*

^b *Department of Civil and Environmental Engineering, University of Cincinnati, PO Box 210071, Cincinnati, OH 45221-0071, USA*

Received 18 March 2002; received in revised form 20 November 2002; accepted 22 November 2002

Abstract

This study presents the cyclic behavior of two types of semi-rigid double web angle connections: bolted-bolted (angles bolted to the beam web and column flange) and welded-bolted (angles welded to beam web and bolted to column flange), with their bolts pretensioned to the proof load. Twenty test specimens were prepared and cyclic load was applied to each test specimen using load control at the beginning cycles, which was converted to displacement control in subsequent cycles upon yielding of angles or bolts materials. The moment–rotation hysteresis loops and the failure modes for all the test cases are presented. The failure modes for bolted-bolted test specimens, depending on angle thickness, were either excessive rotation or beam web bearing, and for the welded-bolted specimens were excessive rotation or bolt fracture. The stiffness, strength, and ductility of the tested connections are compared to those of flush end-plate moment connections reported in literature.

© 2003 Elsevier Science Ltd. All rights reserved.

Keywords: Steel connections; Semi-rigid connections; Cyclic; Dynamic; Hysteresis; Moment–rotation; Energy dissipation; Damping mechanism; Pinching

1. Introduction

Shear connections are traditionally designed to transfer shear force from beams to connecting columns with their bolts being *bearing type* for which high slip resist-

* Corresponding author.

E-mail address: abolmaali@ce.uta.ed (A. Abolmaali).

Nomenclature

b_d	Bolt diameter
b_p	End-plate width
d	Beam depth
G	Distance from heel of the angle to the centerline of first bolt row connected to column flange
g_c	Column gauge
K_e	Connection initial stiffness
l	Angle length used for double web angle connections test specimens
M_u	Connection ultimate moment
t	Angle thickness
t_f	Column flange thickness
t_p	End-plate thickness
p_b	Bolt pitch
p_f	Flange pitch
θ_u	Ultimate connection rotation

ance at service load is not required. These bolts ensure relative rotation of the beam end with respect to the column end, which results in insignificant transfer of moment. Typical examples of shear connections are: single plate, single web angle, double web angle, and top and seat angle connections. Moment connections, on the other hand, transfer moment from the beam end to the column, and the bolts used in these connections are *slip critical* which requires high slip resistance at service load. Some examples of moment connections are the family of end-plate connections such as flush end-plate connection and unstiffened or stiffened extended end-plate connection. In general, bolted or welded-bolted connections, with slip critical bolts, which are pretensioned to 70% of their minimum tensile strength [1], are known as semi-rigid connections.

Among earlier studies during 1940's, Johnson and Green [2] performed 20 tests on welded beam-to-beam and beam-to-column connection by using double web angle and top and seat angle connections. These tests consisted of both pull-out and full scale connection tests in which the test specimens were subjected to repeated loads. The angle and weld return length were the two main variables in these series of tests, and the test results indicated that after completing cycles of fifty-load repetition at 20% above design rotation, each connection continued to take increasing moment until rotation of more than three times the full simple beam rotation were reached without complete failure. Munse et al. [3] conducted three static tests on double web angle connections riveted to beam web and bolted to column flange and one test (the control test) with angles riveted to both beam web and column flange. The test results revealed that the connections, although assumed simple, provide some end resistance, and the resistance provided by the connection increased by using high

strength bolts in lieu of rivets as compared to all riveted connection. This study further reports that the moment–rotation behavior observed in testing was non-linear upon yielding of angle materials. Later Lipson [4] conducted a comprehensive static testing program on single web angle and single plate connections using A325 bolts. The test specimens included: (1) “bolted-bolted” single angle, bolted to beam web and supporting member; (2) “welded-bolted” single angle, welded to supporting member and bolted to the beam web; and (3) “welded-bolted plate”, welded to supporting member and bolted to beam web. Pure moment and moment-shear type tests were conducted, and it was reported that moment–rotation relations for all the test specimens were non-linear in nature from early stages of loading, and rotations in the order of 0.05 rad were observed for most of the test specimens.

Among other studies, the monotonic, cyclic, and dynamic behaviors of different types of semi-rigid connections were investigated in Refs. [5–16]; and it was reported that these connections are capable of dissipating energy because of their relatively “fat” moment–rotation hysteresis loops, which act as damping mechanisms in steel frame structures. Limited cyclic tests were conducted on welded-bolted double web angle connections (DWAC) [17], which showed that significant amount of moment was transferred from the beam end to the column. Liu and Astanah [18] studied the behavior of simple connections subjected to cyclic loads considering the effect of floor slab. This study reported the results of the first series of eight full-scale cyclic tests of shear tab connections bolted to the beam web and welded to the column flange. Specimens without slab were also tested to establish the basic characteristics and behavior of each shear tab connection on its own. It was shown that the addition of the floor slab to the test specimen resulted in roughly twice the maximum lateral load resistance and at approximately 0.04 rad drift, the composite action of specimens with slab was lost due to damage to concrete along with severe buckling of metal deck. At this point, the behavior of specimen with floor slab reverted toward the behavior of the bare steel specimen.

The cyclic performance of two-bolt flush end-plate connections (one row of two bolts in tension region and one row of two bolts in compression region) was studied [19] for which the selection of the test cases was based on the standards and specifications of the Star Building System, Inc. (a prefabricating steel building corporation). The test results in this study showed non-dissipative hysteresis loops, and the failure modes, in general, were governed by bolt rupture rather than end-plate yielding. The cyclic behavior of four-bolt flush end-plate connections (two rows of two bolts in tension region and two rows of two bolts in compression region) was studied by Hartman [20], which was the continuation of the work done by Schuab [19] for which test cases were selected such that dissipative hysteresis loops were obtained. An experimental investigation of the hysteresis behavior of the top and seat angle semi-rigid connections was conducted [21], the results of which also showed that considerable moment was transferred from beam end to the column. Prediction equations were presented for parameters defining hysteresis loops (initial connection stiffness, K_c ; ultimate moment capacity, M_u ; idealized connection yield moment, M_y ; and ultimate connection rotation, θ_u) as function of geometric variables of top and seat angle connection. Also, three mathematical models (elasto-plastic, bilinear, and

modified bilinear models) were proposed to predict the moment–rotation hysteresis loops of these connections. The application of semi-rigid flush end-plate connections to the seismic design of steel frames was investigated [22] in which flush end-plate moment connections were tested under cyclic loading conditions to simulate seismic response. This study suggests that the use of partial-strength semi-rigid connections may be extended to earthquake resistance design due to ductile response observed in some test specimens, which implies that these connections maybe employed as dissipative zones of moment-resisting frames. A comprehensive analytical investigation on cyclic behavior of bolted connections and their effects on overall frame behavior is introduced in Ref. [23], which models the connection mechanism as a rotational spring with two nodes of identical spatial coordinates (one node connected to beam end and the other to column end). The constitutive relationship (moment–rotation hysteresis) of the connection was introduced as the material non-linearity for the connection element, which was incorporated into a dynamic frame analysis computer program. Several examples of steel frames with semi-rigid joints were analyzed by subjecting them to low, medium, and high frequency earthquake records, and the decay of displacement and force responses with time (damping) for connections with fat hysteresis loops, indicated that semi-rigid connections could be reliable sources for energy dissipation in steel frame structures subjected to seismic loads. There are no studies reported on the cyclic behavior of bolted-bolted DWAC.

In this study, the results of an experimental program is presented, which was carried out to obtain moment–rotation hysteresis loops for test specimens of two types of semi-rigid DWAC; bolted-bolted and welded-bolted. Fig. 1(a) shows the bolted-bolted DWAC with angles being bolted to beam web and column flange, while, in welded-bolted DWAC, as shown in Fig. 1(b), the angles are welded to beam web and bolted to column flange. The test cases were selected such that their connections' geometric variables were varied based on current industry's design standards. The test matrix included 12 and 8 test specimens for bolted-bolted and welded-bolted DWAC, respectively. Similar test set up and instrumentations, cyclic loading history, and testing procedures were employed for all the test specimens. The test results include moment–rotation hysteresis loops, which exhibited dissipative loops (fat loops) for most welded-bolted test specimens. The hysteresis loops for bolted-bolted test specimens indicated moderately dissipative loops and beam web bearing behavior for angle thickness of less than 3/8 in. and greater than 3/8 in., respectively. The failure modes were consistent with the behavior and shape of hysteresis loops for each test specimen, and, in general, three failure modes were detected: (1) excessive angle yielding, which was observed for test specimens with relatively low angle thickness compared to their bolt diameter for all welded-bolted and some bolted-bolted connections; (2) bolt fracture, which was observed in test specimens of welded-bolted connections with relatively thick angle as compared with their bolt diameter (none of the test specimens of bolted-bolted connections failed due to this failure mode); and (3) beam web bearing failure, which was only observed for the bolted-bolted test specimens with their angle thickness greater than 3/8 in.

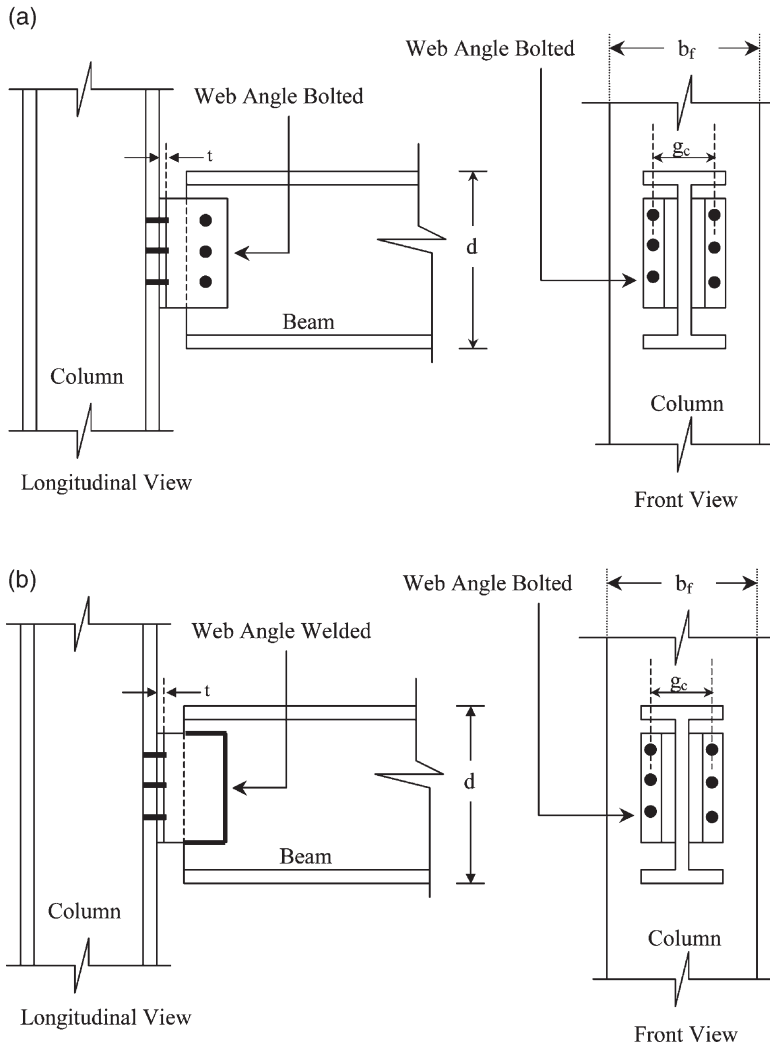


Fig. 1. Configuration of DWAC tested: (a) bolted-bolted; (b) welded-bolted.

2. Experimental program

A typical test set up consisted of a beam, which was connected to a stub-column by means of a semi-rigid connection. The stub-column section was attached to a reaction frame that extended to the base of the laboratory floor. The basic configuration of a typical test set up, a test specimen, and instrumentation are shown in Fig. 2, which consisted of: (1) an actuator to apply the force; (2) a beam of a reaction frame; and (3) two columns of the reaction frame to support a typical test specimen column and the actuator swivel assembly. Lateral braces were provided at the beam

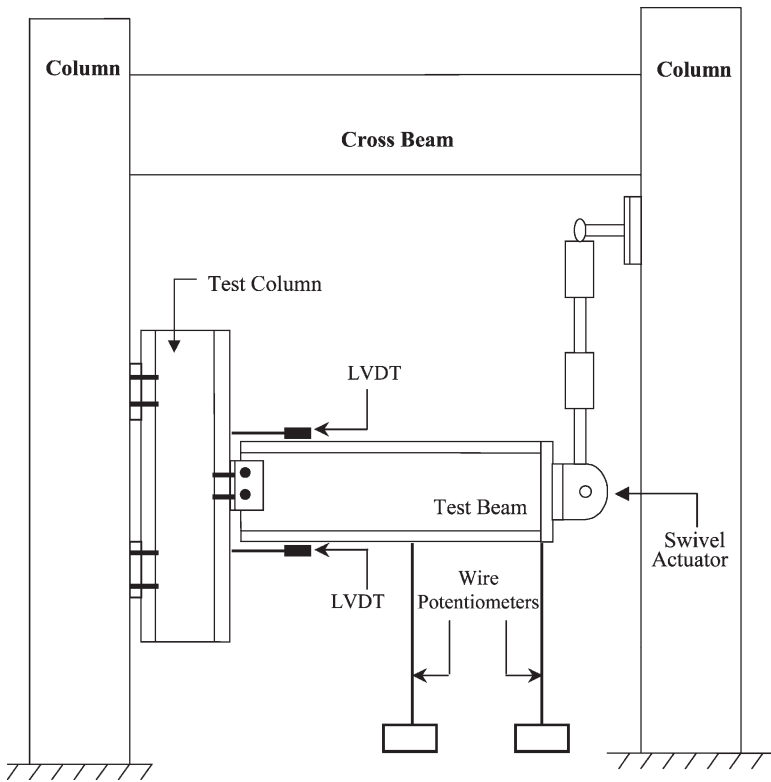


Fig. 2. Typical test set up and instrumentation.

end connected to the actuator swivel to prevent out-of-plane buckling of the test beam. The instrumentation consisted of two Linear Variable Displacement Transducers (LVDTs) to calculate the relative local connection rotation, two wire potentiometers to measure displacements at two points along the beam specimen span (to be used for global rotation calculation), and strain gauged bolts to measure bolt forces. In addition, a load cell and displacement transducers were installed in the actuator to measure the cyclic load applied to the beam-end and the actuator stroke (displacement), respectively. The two LVDTs were placed just above and below the top and bottom beam flanges such that their tips touched the column flange as shown in Fig. 2.

The relative displacements of the two LVDTs divided by the vertical distance between their tips give the local rotation of the connection test specimen. The global rotation of the connection was calculated by dividing the vertical displacement recorded by each wire potentiometer by the distance of the wire potentiometer from the face of the specimen column flange. Hence, the connection rotation at every load level was measured in two independent ways; using LVDT readings and wire potentiometer readings, and the two results were compared for consistency. The moment applied on the connection was calculated by multiplying the force recorded

by the actuator load cell by the distance from the center of the actuator to the face of the column. This typical moment arm distance was about 70 in. depending on the type of the test specimen used.

The test cases selected for bolted-bolted DWAC, which is reported in column two of Table 1 are designated by DW-BB- l - t - b_d - g_c - N - d , where: DW represents the Double Web angle connection, BB stands for bolted-bolted, and l , t , b_d , g_c , N , and d are defined as angle length, angle thickness, bolt diameter, column gauge, number of bolt rows, and beam depth, respectively. Therefore, Test 1 in Table 1, which is designated as DW-BB-102-6-19-114-3-406, denotes a double angle test specimen that is bolted to both the beam web and the column flange, and consists of $102 \times 102 \times 6$ angles with three 19 mm diameter bolts at a column gauge of 119 mm. Similarly, the test cases selected for welded-bolted DWAC are reported in column two of Table 2 and designated by DW-WB- l - t - b_d - g_c - N - d , where WB stands for welded-bolted, and all other variables as defined previously. The beams and columns used for all the test specimens (bolted-bolted and welded-bolted) were W410 \times 67 and W200 \times 100, respectively. The column flange thickness for W200 \times 100 is 24

Table 1
Test cases selected for bolted-bolted DWAC

Test no. (1)	Test Designation DW-BB- l - t - b_d - g_c - N - d (2)	l (mm) (3)	t (mm) (4)	b_d (mm) (5)	g_c (mm) (6)	N (7)	d (mm) (8)
1	DW-BB-102-6-19-114-3-406	102	6	19	114	3	406
2	DW-BB-102-6-19-114-4-406	102	6	19	114	4	406
3	DW-BB-102-16-19-114-4-406	102	16	19	114	4	406
4	DW-BB-102-6-19-114-5-533	102	6	19	114	5	533
5	DW-BB-102-10-19-114-5-533	102	10	19	114	5	533
6	DW-BB-102-10-19-114-3-406	102	10	19	114	3	406
7	DW-BB-102-10-19-114-4-406	102	10	19	114	4	406
8	DW-BB-127-13-16-114-5-610	127	13	16	114	5	610
9	DW-BB-127-19-19-114-5-610	127	19	19	114	5	610
10	DW-BB-102-13-19-114-4-610	102	13	19	114	4	610
11	DW-BB-127-10-16-114-4-610	127	10	16	114	4	610
12	DW-BB-127-10-16-114-6-610	127	10	16	114	6	610

Table 2

Test cases selected for welded-bolted DWAC

Test no. (1)	Test designation g_c-N-d (2)	DW-WB- $l-t-b_d-l$ (mm) (3)	t (mm) (4)	b_d (mm) (5)	g_c (mm) (6)	N (7)	d (mm) (8)
1	DW-WB-76-6-13-64-3-610	76	6	13	64	3	610
2	DW-WB-76-13-19-89-4-610	76	13	19	89	4	610
3	DW-WB-102-16-19-89-5-610	102	16	19	89	5	610
4	DW-WB-102-10-19-89-4-610	102	10	19	89	4	610
5	DW-WB-127-19-19-140-4-610	127	19	19	140	4	610
6	DW-WB-127-13-16-114-6-610	127	13	16	114	6	610
7	DW-WB-152-19-19-191-5-610	152	19	19	191	5	610
8	DW-WB-152-13-22-140-6-610	152	13	22	140	6	610

mm, which was selected to ensure that column rotation would not add significant rotation to overall connection rotation.

The welding process used for the welded-bolted DWAC was Metal Inert Gas (MIG) welding with Lincoln Brand wire of 0.045 in. diameter (Outershield 71 M).

3. Loading history

The initial portion of cyclic loading history applied to all the test specimens is shown in Fig. 3. Each specimen was first loaded to 4.45 kN load applied by the actuator in tension. Then, the specimen was unloaded and reverse loading was applied to a negative value of 4.45 kN actuator load in compression, and finally reloaded to zero. This process was defined as the 4.45 kN loop. For each specimen, three cycles of such 4.45 kN loops were applied at the beginning of the test. Next, the specimen was subjected to three cycles of 8.9 kN loops. The third load step

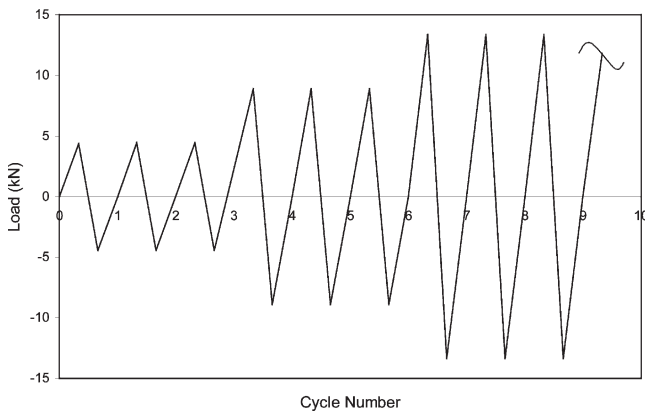


Fig. 3. Loading history under load control.

consisted of applying three cycles of 13.35 kN loops, followed by two cycles of 17.78 kN loops. This process was repeated during the early stages of the test, and during this stage load feedback was used to control the actuator. The value of K_e was computed from the recorded moment–rotation history for these elastic cycles. The load control was continued until a difference in the rotation at peak values in tension and compression was noticed. At this point, the control was switched to displacement control, and the displacement was incremented at 2.5 mm intervals. This increment of 2.5 mm continued until a 25 mm displacement value was reached, then the increment was changed to 5 mm. This displacement increment continued until failure was reached.

4. Test results

4.1. Bolted-bolted double web angle connection

Twelve tests were conducted for bolted-bolted DWAC for which the details of their geometric variables are presented in Table 1. Two failure modes were observed to occur: excessive rotation and beam web bearing failure. Excessive rotation of connection mechanism normally occurs due to excessive yielding of the angle material beyond acceptable rotation limits (normally 0.03–0.05 rad for semi-rigid connections), which causes significant loss in connection stiffness. The testing was stopped when any further increase in load cycles did not result in much gain in strength (i.e. moment), but it led to a very rapid increase in rotation. The other type of failure observed was beam web bearing failure, which occurred on test specimens with angle thickness $t > 10$ mm. The reason for this failure is that as angle thickness increases, the moment resistance of the connection increases. The resulting larger moment causes larger forces to be transferred to the beam web bolts as shear forces. This transfer of higher bolt shear forces cause the beam web material around the bolt holes to fail in bearing, which can be observed by the holes becoming oval shaped.

Table 3 summarizes the values of K_e , M_u , and θ_u along and their respective failure modes for each of the twelve bolted-bolted test specimens. The test results presented in column two show that the lowest and highest connection stiffness was recorded for Test 1 ($K_e = 1889$ (kN m)/rad) and Test 9 ($K_e = 35,482$ (kN m)/rad), respectively. Comparison of angle thickness for Test 1 ($t = 6$ mm) and Test 9 ($t = 19$ mm) shows that increasing angle thickness, as expected, increases the connection initial stiffness. In addition, in Test 9 the number of bolt rows was, $N = 5$, whereas, in Test 1, the number of bolt rows was, $N = 3$, which indicates that more angle materials was used for Test 9 than those for Test 1, which also contributes to higher initial stiffness for Test 9.

The test results presented in column four of Table 3 show that the lowest and highest values for ultimate moment was obtained for Test 1 ($M_u = 12$ kN m) and Test 12 ($M_u = 93$ kN m), respectively, and the next highest value of ultimate moment is observed for Test 9 ($M_u = 92$ kN m). Comparison of the connection variables for these tests shows that Test 1 has the lowest value of angle thickness ($t = 6$ mm) and

Table 3
Test results for bolted-bolted DWAC

Test no. (1)	Test designation DW-BB- <i>l-t-b_d-g_c-N-d</i> (2)	Initial stiffness K_e ((kN m)/rad) (3)	Ultimate moment M_u (kN m) (4)	Ultimate rotation θ_u (rad) (5)	Failure mode (6)
1	DW-BB-102-6-19-114-3-406	1889	12	0.0500	Angle yielding
2	DW-BB-102-6-19-114-4-406	2966	21	0.0500	Angle yielding
3	DW-BB-102-16-19-114-4-406	18,649	63	0.0500	Web bearing
4	DW-BB-102-6-19-114-5-533	11,187	33	0.0500	Angle yielding
5	DW-BB-102-10-19-114-5-533	21,990	61	0.0500	Angle yielding
6	DW-BB-102-10-19-114-3-406	6074	19	0.0500	Angle yielding
7	DW-BB-102-10-19-114-4-406	13,812	39	0.0500	Angle yielding
8	DW-BB-127-13-16-114-5-610	19,268	80	0.0450	Web bearing
9	DW-BB-127-19-19-114-5-610	35,482	92	0.0450	Web bearing
10	DW-BB-102-13-19-114-4-610	12,204	50	0.0450	Web bearing
11	DW-BB-127-10-16-114-4-610	5690	37	0.0450	Yielding/bearing
12	DW-BB-127-10-16-114-6-610	17,854	93	0.0450	Angle yielding

Test 9 has the highest ($t = 19$ mm), but the maximum value of ultimate moment was recorded for Test 12 ($M_u = 93$ kN m) with angle thickness, $t = 10$ mm. By careful examination of number of bolt rows for Test 9 $N = 5$ and Test 12 ($N = 6$), it can be concluded that as the number of bolt rows increases in Test 12 (more angle material is used), the ultimate moment of the connection is slightly increased, even though the angle thickness for Test 9 is greater than that of Test 12.

Column five of Table 3 presents the values of ultimate rotation recorded for the test specimens of bolted-bolted connections, which varied from of 0.045–0.05 rad. The failure modes for test specimens of this series of tests are tabulated in column six of Table 3, which shows that Tests 1, 2, 4 through 7, and 12 exhibited angle yielding that indicates the failure was governed by excessive yielding of the angle material, resulting in excessive rotation. In Tests 3 and 8 through 10, the failure of the connections were bearing failure of beam web material due to bolt bearing against the beam web and causing elongation (egging) of the bolt holes. In Test 11, a mixed failure mode was observed.

The moment–rotation hysteresis loops for Tests 1 through 12 of bolted-bolted

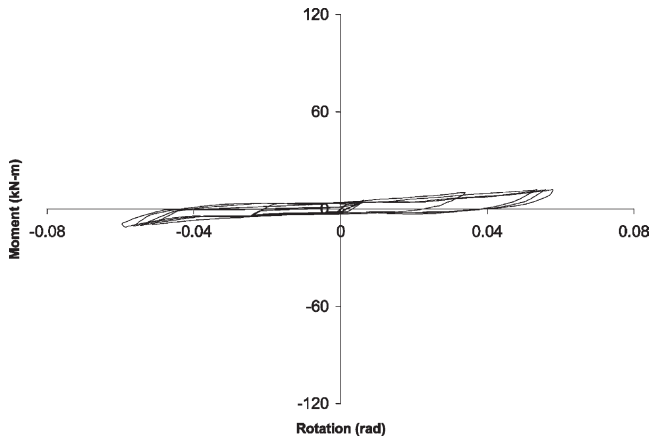


Fig. 4. Moment–rotation hysteresis loops for DW-BB-102-6-19-114-3-406.

DWAC are presented in Figs. 4–15, respectively. As can be seen from the overall shapes of hysteresis loops obtained, all tests exhibited significant cyclic yielding, which resulted in increasing rotation with increasing load with different degrees of pinching. Pinching results from the permanent deformation caused in the yielded materials, which is unrecoverable during load reversal. Both the angle material and bolt shank yield in the connection as the load cycles are increased. Due to excessive yielding of the angle material, the surface area of contact between the angle leg and the column flange would decrease in subsequent load reversals. This would lead to increased bolt forces in the bolts connecting the angle legs to the column flange, and ultimately causes yielding in the bolt shanks, which would then lead to unrecoverable permanent deformation in the bolt shank and a gap between the angle and column flange. By referring to Figs. 6, 11–13 for Tests 3, 8, 9, and 10 (test specimens with

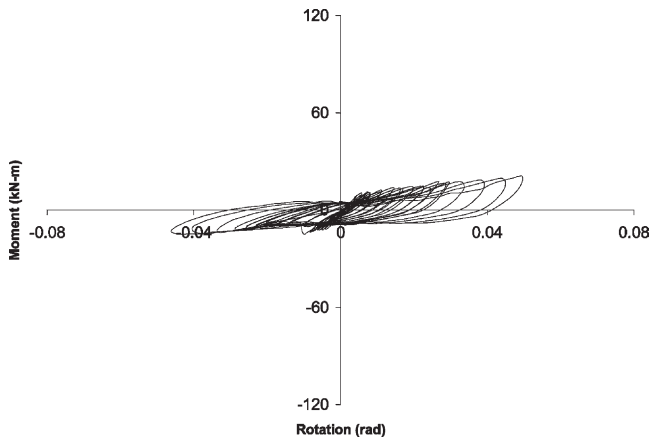


Fig. 5. Moment–rotation hysteresis loops for DW-BB-102-6-19-114-4-406.

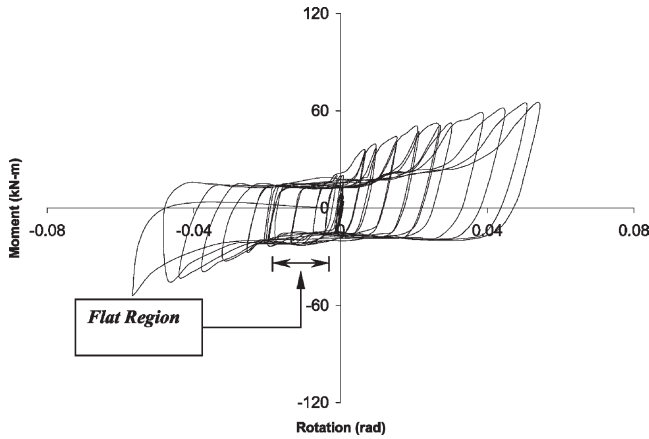


Fig. 6. Moment–rotation hysteresis loops for DW-BB-102-16-19-114-4-406.

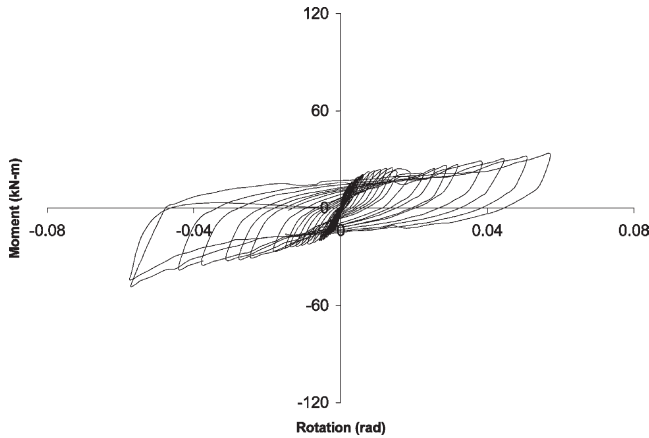


Fig. 7. Moment–rotation hysteresis loops for DW-BB-102-6-19-114-5-533.

beam web bearing failure), respectively, it can be seen that the overall shape of each hysteresis loops have a “flat” region in the vicinity of the origin of moment and rotation axes, which is the landmark of such failure. Since, this failure causes elongation of the beam web’s bolt-holes (change in geometrical configuration of bolt holes from circular to oval shape), it assists the bolts to move freely in the bolt-holes during load reversal, which induces the flat regions on the hysteresis loops.

4.2. Welded-bolted double web angle connection

Eight test specimens were selected and tested for welded-bolted DWAC, geometric details of which are presented in Table 2. The failure modes observed were either excessive rotation caused by angle yielding or bolt fracture. Columns 3–5 of Table

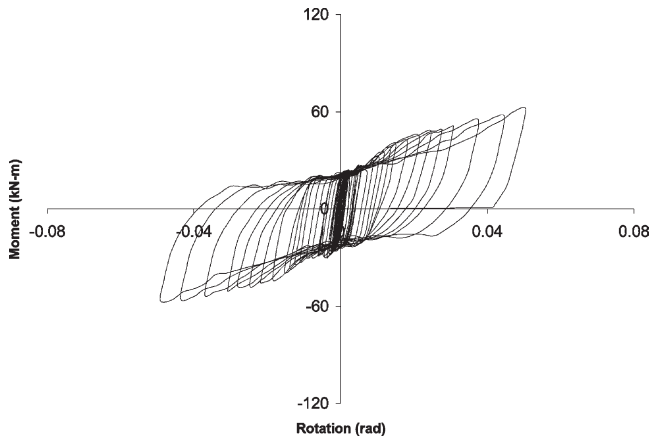


Fig. 8. Moment–rotation hysteresis loops for DW DW-BB-102-10-19-114-5-533.

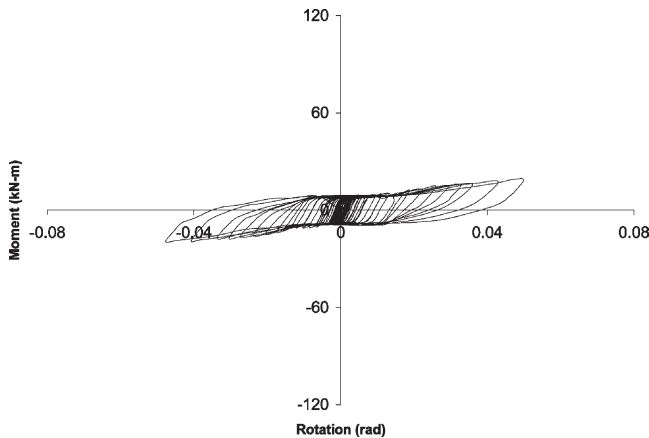


Fig. 9. Moment–rotation hysteresis loops for DW-BB-102-10-19-114-3-406.

4 summarize the values of K_e , M_u , and θ_u obtained for these eight tests, respectively. The lowest and highest values of K_e were obtained from Test 1 (5406 (kN m)/rad) and Test 3 (54,669 (kN m)/rad), respectively, similarly, the lowest and highest values of M_u was obtained from Test 1 (29 kN m) and Test 3 (253 kN m), respectively. By referring to column five, The values of θ_u varied from 0.0228–0.0395 rad for Tests 3 and 4 (or 5), respectively. These values of ultimate rotations are directly related to the mode of failure of each test specimen reported in column six of Table 4, which include either angle yielding, bolt fracture, or a combination of angle yielding and bolt fracture. The mode of failure for Test 1 ($\theta_u = 0.0315$ rad) was a combination of angle yielding and bolt fracture, for Test 3 ($\theta_u = 0.0228$ rad) was bolt fracture, and for Tests 2 and 4 through 8, with $\theta_u > 0.0300$ was angle yielding. Therefore, any test specimen with an ultimate rotation of $\theta_u > 0.0300$ exhibited angle yielding

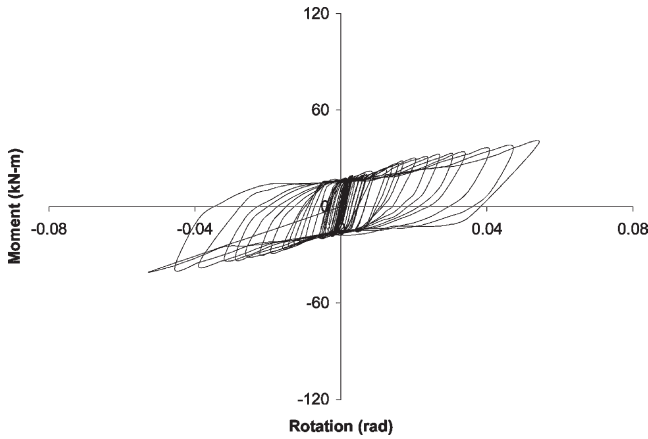


Fig. 10. Moment–rotation hysteresis loops for DW-BB-102-10-19-114-4-406.

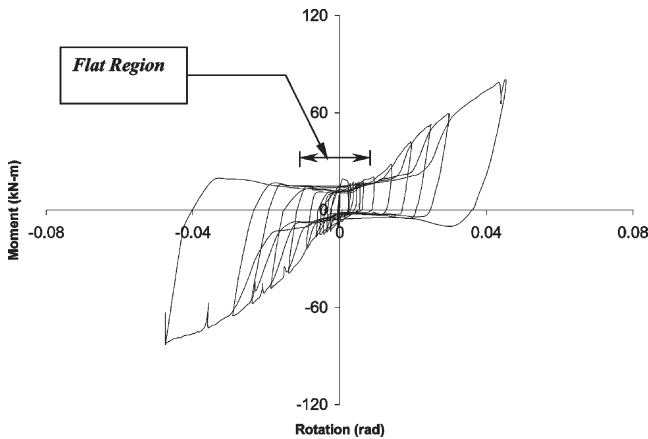


Fig. 11. Moment–rotation hysteresis loops for DW-BB-127-13-16-114-5-610.

behavior and the testing process was terminated manually. On the other hand, the ultimate rotation of $\theta_u < 0.0300$ indicated bolt fracture prior to excessive rotation due to angle yielding.

The moment–rotation hysteresis loops obtained for welded-bolted DWAC are presented in Figs. 16–23. Visual inspection of these figures indicates that Test 1 (refer to Fig. 16) has the lowest energy dissipating capacity and Test 8 (refer to Fig. 23) has the highest. Hysteresis loops of Test 3 (Fig. 18) shows that testing was stopped at $\theta = 0.0228$ rad due to bolt fracture. It is evident from these figures that hysteresis loops for all the test specimens exhibited different degrees of pinching, which was due to angle yielding and separation from column flange.

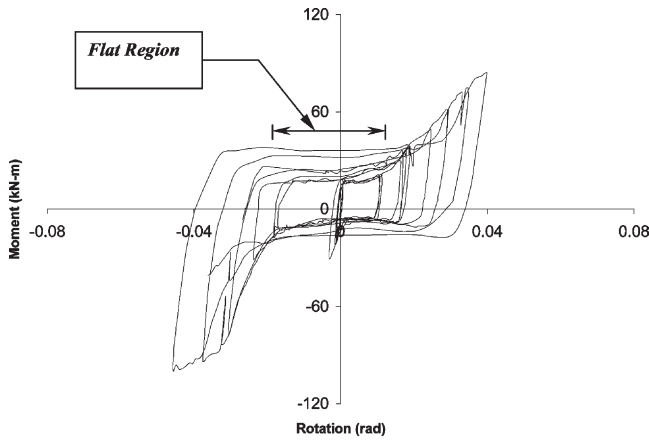


Fig. 12. Moment–rotation hysteresis loops for DW-BB-127-19-19-114-5-610.

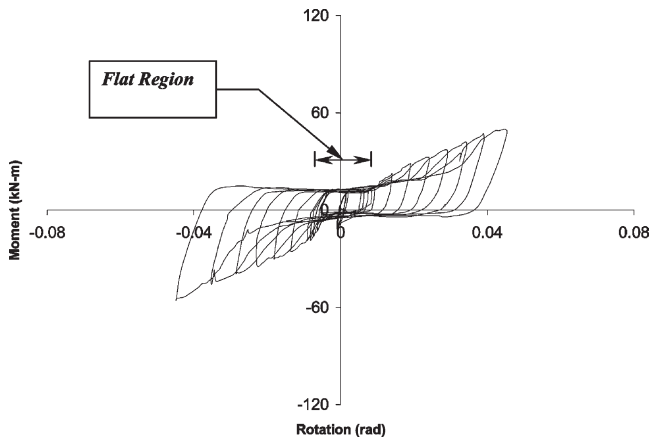


Fig. 13. Moment–rotation hysteresis loops for DW-BB-102-13-19-114-4-610.

4.3. Comparison with traditional moment connections

As mentioned earlier, in structural engineering practice, DWAC are normally designed as shear connections with their bolts snug-tight. The bolts of semi-rigid DWAC, on the other hand, are normally pretensioned to their proof load level (the type of DWAC used in this study). Even though it seems inept, it is interesting to compare the cyclic behavior of semi-rigid DWAC of this study and those of the flush end-plate semi-rigid connection, which are traditionally designed as moment connections in steel buildings. The cyclic test results of the four-bolt flush end-plate connections (FBFEPC) investigated by Hartman [20] are considered for this purpose, the geometric configuration of which is shown in Fig. 24. The selection of these test cases was based on the FBFEPC commonly used and identified by prefabricating

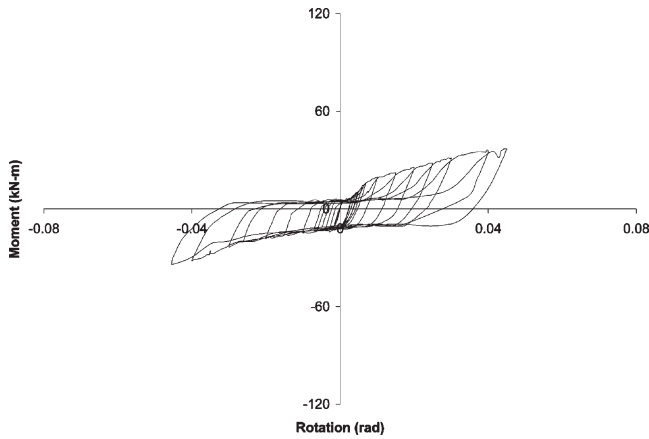


Fig. 14. Moment–rotation hysteresis loops for DW-BB-127-10-16-114-4-610.

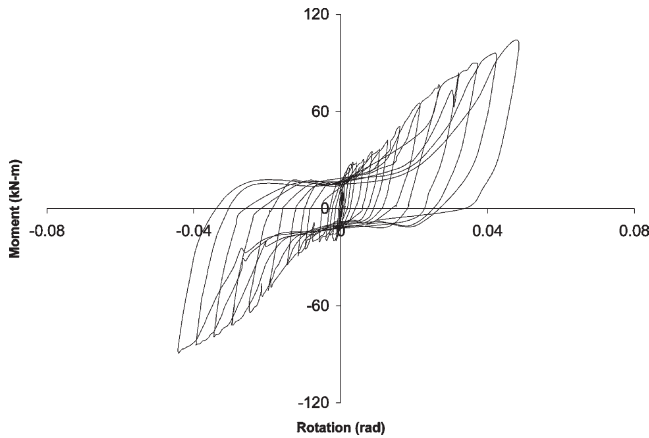


Fig. 15. Moment–rotation hysteresis Loops for DW-BB-127-10-16-114-6-610.

building industries. Table 5 summarizes the values of the geometric variables for the nine test specimens selected. The FBFEPCC test specimens reported in column two of Table 5 are designated by FEP-4B- b_p - d_p - t_p - b_d - p_f - p_b - g_c , where FEP represents the flush end-plate connection and 4B represents two rows of two bolts on tension side and two rows of two bolts on compression side of the beam flanges; b_p , d_p , t_p , b_d , p_f , p_b , and g_c are defined as end-plate width, end-plate depth, end-plate thickness, bolt diameter, flange pitch, bolt pitch, and column gauge, respectively. Hence, a test specimen designated as FEP-4B-152-457-13-19-41-76-76 is interpreted as a flush end-plate connection with two rows of bolts on compression and tension sides of the beam flanges with: end-plate width, $b_p = 152$ mm; end-plate depth, $d_p = 457$ mm; end-plate thickness, $t_p = 13$ mm; bolt diameter, $d_p = 19$ mm; flange pitch, $p_f = 41$ mm; bolt pitch, $p_b = 76$ mm; and column gauge, $g_c = 76$ mm.

Table 4
Test results for welded-bolted DWAC

Test no. (1)	Test designation b_d-g_c-N-d (2)	Initial stiffness K_e ((kN m)/rad) (3)	Ultimate moment M_u (kN m) (4)	Ultimate rotation θ_u (rad) (5)	Failure mode (6)
1	DW-WB-76-6-13-64-3-610	5406	29	0.0315	Angle yielding/bolt fracture
2	DW-WB-76-13-19-89-4-610	28,538	120	0.0369	Angle yielding
3	DW-WB-102-16-19-89-5-610	54,699	253	0.0228	Bolt fracture
4	DW-WB-102-10-19-89-4-610	32,263	93	0.0395	Angle yielding
5	DW-WB-127-19-19-140-4-610	16,254	142	0.0395	Angle yielding
6	DW-WB-127-13-16-114-6-610	44,600	206	0.0320	Angle yielding
7	DW-WB-152-19-19-191-5-610	3067	204	0.0376	Angle yielding
8	DW-WB-152-13-22-140-6-610	45,443	202	0.0351	Angle yielding

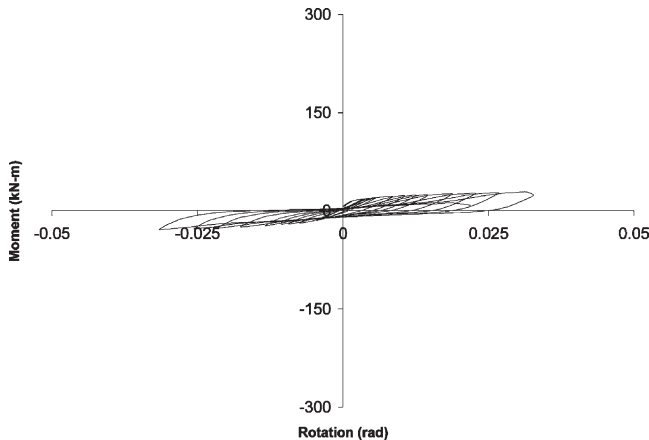


Fig. 16. Moment–rotation hysteresis loops for DW-WB-76-6-13-64-3-610.

Similar test set up, instrumentation, and loading history as the one presented in this study was adopted by Nader and Astaneh-Asl [16]. Table 6 presents the test results for stiffness, strength, and failure mode of each test specimen. The lowest and highest values of K_e were obtained from the results of Test 1 (51,795 (kN m)/rad) and Test 9 (148,205 (kN m)/rad), respectively. Similarly, the lowest and highest values of the M_u were recorded for Test 1 (250 kN m) and Test 9 (554 kN m). Finally, the values of θ_u varied from 0.0007–0.0188 rad for Tests 2 and 4, respectively. Comparing these values of θ_u for FBFEPCC with those observed for DWAC (refer to Tables 3 and 4), it is evident that, in general, much smaller ultimate rotations

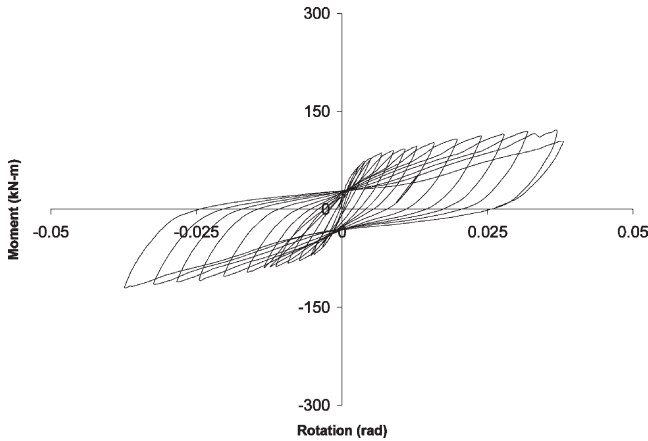


Fig. 17. Moment–rotation hysteresis loops for DW-WB-76-13-19-89-4-610.

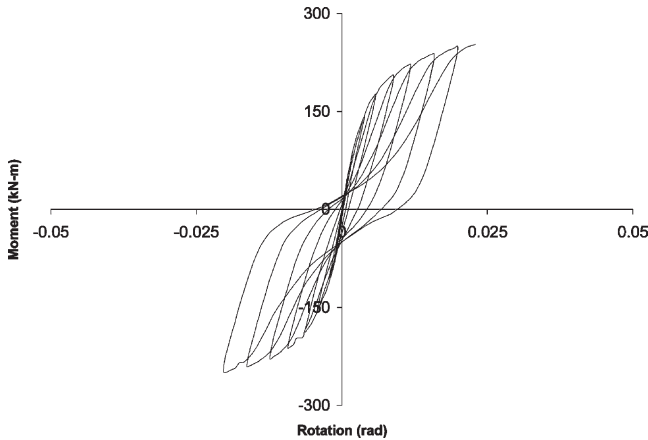


Fig. 18. Moment–rotation hysteresis loops for DW-WB-102-16-19-89-5-610.

were obtained for test specimens of FBFEPc. The failure modes for these test specimens are listed as either plate rupture or bolt fracture, in column six of Table 6. The plate rupture was defined by Hartman [20] to occur when the end-plate ruptured along the weld line of the beam web. The failure categorized as bolt fracture is bolt rupture in tension, and it was reported in Ref. [20] that bolt fracture for all the test specimens of FBFEPc was accompanied by end-plate yielding.

When comparing cyclic performance (refer to Tables 3 and 4) of the semi-rigid DWAC studied here with those of the FBFEPc [20] of Table 6, it is interesting to note that the value K_e for Test 3 (54,699 (kN m)/rad) of welded-bolted DWAC is almost equal to that for Test 2 of FBFEPc (56,311 (kN m)/rad). Similarly, the value of M_u , for Test 3 (253 kN m) of DWAC is almost equal to that of Test 2 (252 kN m) of FBFEPc. This observation shows that semi-rigid DWAC can be designed to pro-

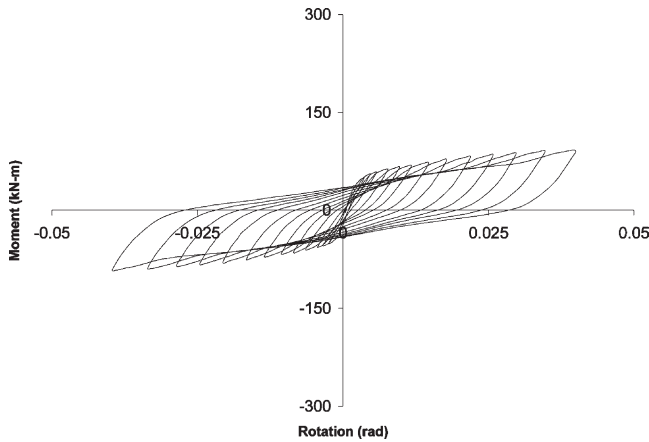


Fig. 19. Moment–rotation hysteresis loops for DW-WB-102-10-19-89-4-610.

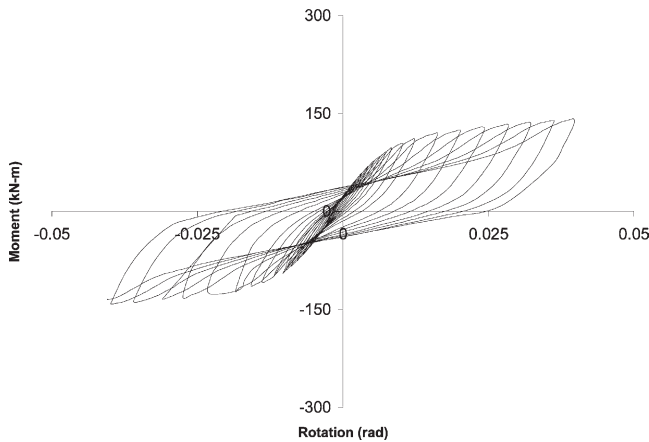


Fig. 20. Moment–rotation hysteresis loops for DW-WB-127-19-19-140-4-610

vide comparable stiffness and strength as those of some moment connections. Moreover, comparing the values of θ_u indicated that $\theta_u = 0.0228$ rad for Test 3 of welded-bolted DWAC, whereas, $\theta_u = 0.0121$ rad for Test 2 of FBFEPc (almost twice larger). This indicates that Test 3 of DWAC behaves more ductile than the Test 2 of flush end-plate connection; thus, leading to the conclusion that Test 3 of DWAC provides same stiffness and strength as Test 2 of FBFEPc, and possesses higher ductility. Finally, either end-plate rupture or bolt fracture was the governing failure modes for all the test specimens of FBFEPc tested by Hartman [20], while, excessive yielding, which is a more desirable failure mode, governed most of the test specimens of the welded-bolted DWAC.

Finally, the coupon test results for angles (used for bolted-bolted and welded-bolted DWAC) and plates (used for flush end-plate) are presented in Table 7. The

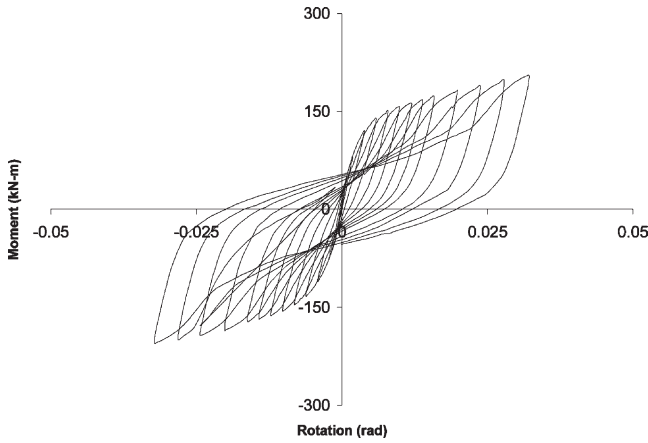


Fig. 21. Moment–rotation hysteresis loops for DW-WB-127-13-16-114-6-610

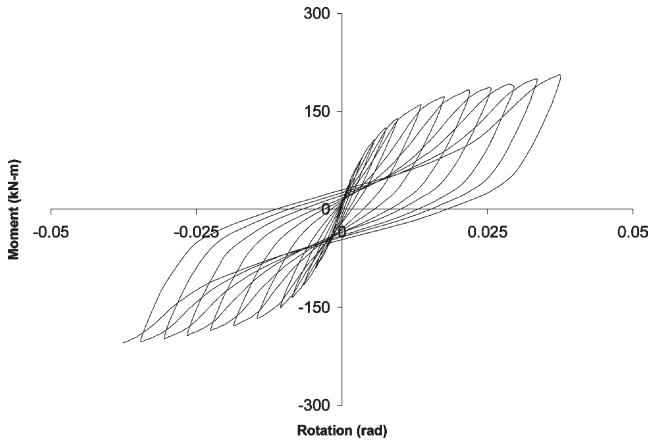


Fig. 22. Moment–rotation hysteresis loops for DW-WB-152-19-19-191-5-610

coupon tests for the beam and column materials were not performed since they were selected to remain elastic throughout the testing in order to force yielding/failure in the connection mechanism.

5. Application of moment–rotation hysteresis loops in dynamic analysis of frames

In dynamic analysis of steel frames with semi-rigid or partially restrained connections (PR), each connection mechanism is typically modeled as a two noded non-linear rotational spring element [24], which has zero length, and the ends of which experience, the same translation displacements along the global Cartesian axis, but

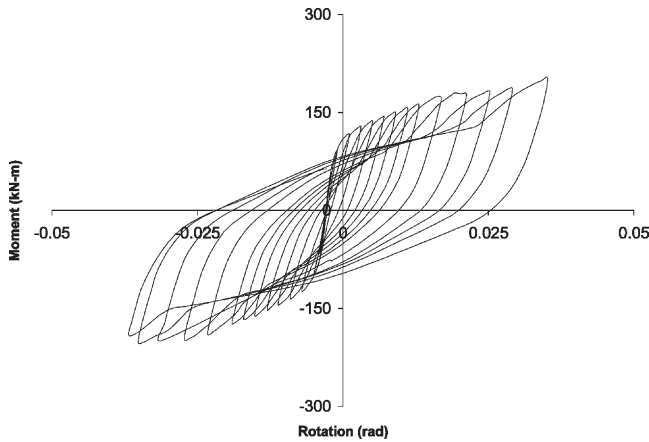


Fig. 23. Moment–rotation hysteresis loops for DW-WB-152-13-22-140-6-610

different rotations (refer to Fig. 25(a)). Thus, the degrees-of-freedom for both the end nodes of this spring element must be identical for the x and y translations, but different for rotational degrees-of-freedom. For example, for the node numbering scheme shown in Fig. 25(b), if the left column top-end node degrees-of-freedom numbers are 1, 2, 3; then, the node number for the beam-end the degrees-of-freedom numbers will be 1, 2, 4. The experimentally obtained cyclic moment–rotation hysteresis loops (such as the ones obtained in this study) are used as material non-linearity for the PR connection element, which enforces non-linear dynamic analysis. In the non-linear solution algorithm, the differential equations of motion for the discretized system are solved in its original form by subdividing the total time into equal size time steps, and assuming an appropriate acceleration variation in each time step. An iterative algorithm is necessary to predict the response at the end of each time step, and a Newton–Raphson type scheme is employed to march along the non-linear moment–rotation hysteresis loops of each connection in each iterative cycle. Detailed algorithms and discussion of non-linear static and dynamic analysis of steel frames with PR joints along with their convergence criteria are presented by the first author of this paper in Ref. [24].

6. Conclusion

The cyclic behavior of bolted-bolted and welded-bolted semi-rigid DWAC is presented in this paper for selected test cases. An experimental testing program was carried out for which each test specimen consisted of a beam connected to a column using a DWAC. The column flanges for each test specimen was selected such that they did not contribute to overall connection rotation. A load control cyclic load history was applied to each test specimen up to its elastic response, and control was switched to displacement control during inelastic behavior of subsequent loading

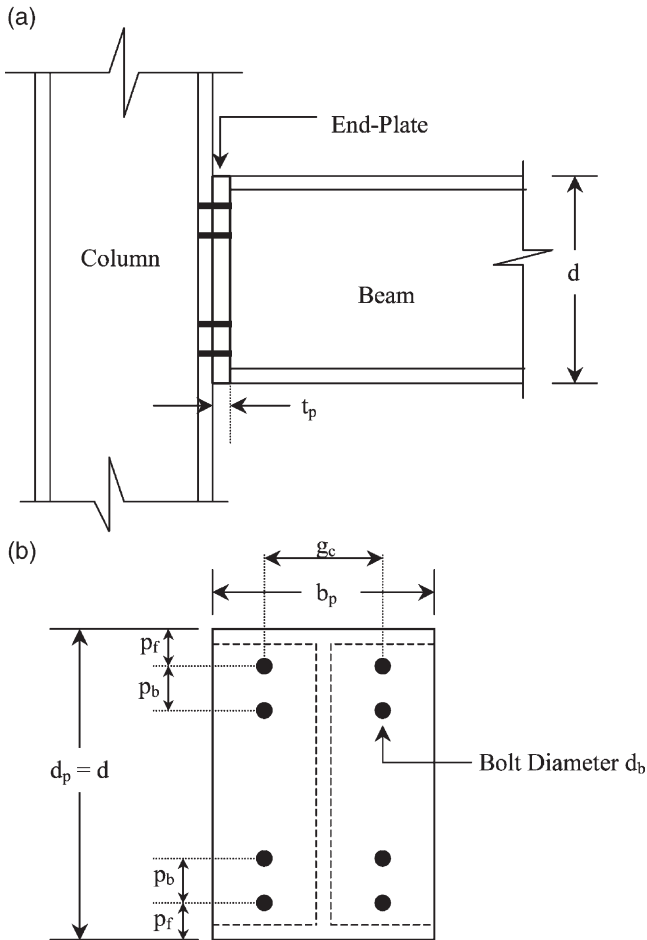


Fig. 24. Configuration of the flush end-plate connection tested by Hartman [20]: typical side view; (b) typical front view.

cycles. The moment–rotation hysteresis loops are presented for all the test specimens, and the cyclic behavior of each test specimen is discussed. The values of the connection initial stiffness, ultimate moment capacity, ultimate rotation capacity, and failure mode are also presented.

For bolted-bolted semi-rigid DWAC, two failure modes were observed: excessive rotation due to yielding of the angle and beam web bearing failure. The excessive rotation was observed for the test specimens with angle thickness, $t \leq 10$ mm, while the beam web bearing was identified for the test specimens with angle thickness, $t > 10$ mm. The moment–rotation hysteresis loops, in general, exhibited pinching for both failure modes, and for the case of beam web bearing failure, the pinching of the hysteresis loops had a well-defined flat portion. The overall behavior showed that these connections are capable of dissipating energy, and for certain combinations

Table 5
Test cases selected by Hartman [20] for flush end-plate connections

Test no. (1)	Test designation FEP-4B- b_p - d_p - t_p - b_d - p_f - p_b - g_c (2)	b_p (mm) (3)	d_p (mm) (4)	t_p (mm) (5)	b_d (mm) (6)	p_f (mm) (7)	p_b (mm) (8)	g_c (mm) (9)
1	FEP-4B-152-457-13-19-41-76-76	152	457	13	19	41	76	76
2	FEP-4B-152-457-16-19-41-76-76	152	457	16	19	41	76	76
3	FEP-4B-203-457-10-25-48-89-89	203	457	10	25	48	89	89
4	FEP-4B-203-457-13-25-48-89-89	203	457	13	25	48	89	89
5	FEP-4B-152-559-10-19-41-76-76	152	559	10	19	41	76	76
6	FEP-4B-152-559-13-19-41-76-76	152	559	13	19	41	76	76
7	FEP-4B-152-559-16-19-41-76-76	152	559	16	19	41	76	76
8	FEP-4B-203-559-10-25-48-89-89	203	559	10	25	48	89	89
9	FEP-4B-203-559-19-25-48-89-89	203	559	19	25	48	89	89

Table 6
Test results obtained by Hartman [20] for flush end-plate connections

Test no. (1)	Test designation FEP-4B- b_p - d_p - t_p - b_d - p_f - p_b - g_c (2)	Initial stiffness K_e ((kN m)/rad) (3)	Ultimate moment M_u (kN m) (4)	Ultimate rotation θ_u (rad) (5)	Failure mode (6)
1	FEP-4B-152-457-13-19-41-76-76	51,795	250	0.0121	Bolt fracture
2	FEP-4B-152-457-16-19-41-76-76	56,311	252	0.0070	Bolt fracture
3	FEP-4B-203-457-10-25-48-89-89	79,009	255	0.0151	Plate rupture
4	FEP-4B-203-457-13-25-48-89-89	105,690	388	0.0188	Bolt failure
5	FEP-4B-152-559-10-19-41-76-76	67,696	252	0.0098	Plate rupture
6	FEP-4B-152-559-13-19-41-76-76	69,645	313	0.0108	Bolt fracture
7	FEP-4B-152-559-16-19-41-76-76	82,034	327	0.0084	Bolt fracture
8	FEP-4B-203-559-10-25-48-89-89	103,422	324	0.0097	Weld failure
9	FEP-4B-203-559-19-25-48-89-89	148,205	554	0.0140	Bolt fracture

Table 7
Results of coupon tests for angle/plate materials

Bolted-bolted double web angle connection		Welded-bolted double web angle connection		Four bolted flush end-plate connection	
Test no.	Yield stress (MPa)	Test no.	Yield stress (MPa)	Test no.	Yield stress (MPa)
1	316.9	1	305.2	1	358.2
2	303.1	2	359.4	2	372.0
3	344.5	3	400.6	3	365.1
4	392.7	4	393.9	4	337.6
5	358.2	5	327.5	5	351.4
6	303.1	6	339.7	6	361.7
7	289.4	7	399.2	7	378.9
8	316.9	8	343.9	8	350.0
9	399.6			9	392.7
10	330.7				
11	392.7				
12	316.9				

of geometric variables resulted in significant moment transfer across the connection before failure.

For welded-bolted DWAC, the moment–rotation hysteresis loops, showed significant ductility and pinching at higher load levels. The failure modes were: excessive yielding of angles and tensile failure of bolts, and the hysteresis loops were dissipative (“fat loops”). The initial stiffness and moment capacity as high as 54,699 (kN m)/rad and 253 kN m were recorded, respectively. These values were comparable with those obtained for some flush end-plate connections cyclic tests reported in Ref. [16], interestingly, for the same stiffness and strength, the DWAC of this study was more dissipative (more ductility).

These observations made are based on limited test data obtained in this research, hence, authors do not aim to generalize these findings.

Acknowledgements

The financial support of the National Science Foundation (Grant EEC-9820102) for conducting this study is greatly acknowledged.

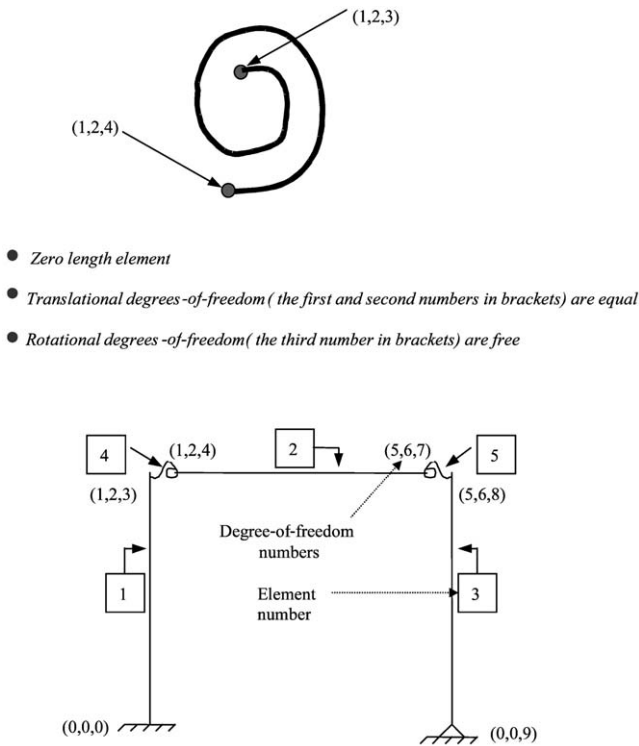


Fig. 25. Semi-rigid connection model: (a) rotational spring element configuration; (b) plane frame discrete model with semi-rigid connection.

References

- [1] American Institute of Steel Construction. Manual of steel construction: load and resistance factor design. 2nd ed. vol. 2; AISC, Chicago, 1994.
- [2] Johnson B, Green L. Flexible welded angle connections, AWS. Weld J 1940;19(10):402–8.
- [3] Munse WH, Bell WG, Chesson E. Behavior of riveted and bolted beam-to-column connections. J Struct Div ASCE 1959;85(ST3):29–50.
- [4] Lipson SL. Single-angle welded-bolted connections. In: Proceedings of the Canadian Structural Engineering Conference, Toronto, Canada. 1968. p. 139–62.
- [5] Popov EP, Bertero P. Cyclic loading of steel beams and connections. J Struct Div ASCE 1973;99(6):1189–204.
- [6] Kukreti AR, Ghassemeh M, Murray TM. Behavior and design of large-capacity moment-endplates. J Struct Eng ASCE 1990;116(3):809–28.
- [7] Kukreti AR, Murray TM, Ghassemieh M. Finite element modeling of large capacity stiffened steel tee-hanger connections. Int J Comput Struct 1989;32(2):409–22.
- [8] Kukreti AR, Abolmaali A. Moment–rotation hysteresis behavior of top and seat angle steel frame connections. J Struct Eng 1999;125(8):810–20.
- [9] Popov EP, Bertero P. Cyclic loading of steel beams and connections. J Struct Eng ASCE 1973;99(ST6):1189–204.
- [10] Popov EP, Pinkey RB. Cyclic loading of steel beams and connections subjected to inelastic strain reversals. Bulletin No. 13, AISI; 1968.

- [11] Popov EP, Bertero V. Cyclic loading of steel beams and connections. *J Struct Eng* 1973;99(ST6):1189–204.
- [12] Sarraf M, Bruneau M. Cyclic testing of existing and retrofitted riveted stiffened seat angle connections. *J Struct Eng ASCE* 1996;122(7):762–75.
- [13] Thomson AW, Broderick BM. Seismic resistance of flush endplate connections. *J Struct Eng* 2000;78(17):28–33.
- [14] Tsai KC, Wu SW, Popov EG. Experimental performance of seismic steel beam-column moment joints. *J Struct Eng* 1995;121(6):925–31.
- [15] Youseff-Agha W, Aktan HM, Olowokere OD. Seismic response of low-rise steel frames. *J Struct Eng* 1989;115(3):594–607.
- [16] Nader MN, Astaneh-Asl A. Shaking table tests of rigid, semirigid, and flexible steel frames. *J Struct Eng* 1996;122(6):589–96.
- [17] Astaneh A, Nader MN, Malik L. Cyclic behavior of double web angle connections. *J Struct Eng ASCE* 1989;115(5):1101–18.
- [18] Liu J, Astaneh-Asl A. Cyclic testing of simple connections including effects of slab. *J Struct Eng ASCE* 2000;126(1):32–9.
- [19] Schuab S. Cyclic behavior of flush end-plate connections. A thesis submitted as partial fulfillment of the requirement for degree of Mater of Science, Department of Civil Engineering, University of Oklahoma, Norman, Oklahoma; 1998.
- [20] Hartman J. Cyclic performance of flush end-plate connections. A thesis submitted as partial fulfillment of the requirement for degree of Mater of Science, Department of Civil Engineering, University of Oklahoma, Norman, Oklahoma; 1999.
- [21] Kukreti AR, Abolmaali A. Moment–rotation hysteresis behavior for top and seat angle connections. *J Struct Eng ASCE* 1999;125(8):810–20.
- [22] Thomson AW, Broderick BM. Seismic resistance of flush end-plate connections. *Proc Inst Struct Eng* 2000;78(17):28–33.
- [23] Kukreti AR, Abolmaali A. Dynamic analysis of steel frames with semi-rigid connections. In: *Proceedings of the XIXII Southeastern Conference on Theoretical and Applied Mechanics*, Deerfield Beach, Florida, May 13–16. 2000.
- [24] Abolmaali A. Nonlinear finite element dynamic analysis of steel frames with flexible joints. PhD dissertation submitted as partial fulfillment for degree of Doctor of Philosophy, School of Civil and Environmental Engineering and Environmental Science, University of Oklahoma, Norman, Oklahoma; 1999.